HHS Public Access

Author manuscript

*Stroke*. Author manuscript; available in PMC 2023 May 01.

Published in final edited form as:

*Stroke*. 2022 May ; 53(5): 1570–1579. doi:10.1161/STROKEAHA.121.035674.

# Oxygen metabolic stress and white matter injury in patients with cerebral small vessel disease

**Peter Kang, MD, MSCI**[1,*], **Chunwei Ying, BS**[3,*], **Yasheng Chen, DSc**[1], **Andria L. Ford, MD, MSCI**[1,2,†], **Hongyu An, DSc**[1,2,3,†], **Jin-Moo Lee, MD, PhD**[1,2,3,†]

[1]Department of Neurology, Washington University School of Medicine

[2]Mallinckrodt Institute of Radiology, Washington University School of Medicine

[3]Department of Biomedical Engineering, Washington University

## Abstract

**Background and Purpose:** Chronic hypoxia-ischemia is a putative mechanism underlying the development of white matter hyperintensities (WMH) and microstructural disruption in cerebral small vessel disease (CSVD). WMH fall primarily within deep white matter watershed regions. We hypothesized that elevated oxygen extraction fraction (OEF), a signature of hypoxia-ischemia, would be detected in the watershed where WMH density is highest. We further hypothesized that OEF would be elevated in regions immediately surrounding WMH, at the leading edge of growth.

**Methods:** In this cross-sectional study conducted from 2016 to 2019 at an academic medical center in St. Louis, Missouri, participants (age >50) with a range of cerebrovascular risk factors underwent brain MRI using pseudocontinuous arterial spin labeling, asymmetric spin echo, FLAIR and diffusion tensor imaging (DTI) to measure cerebral blood flow (CBF), OEF, WMH, and white matter (WM) integrity, respectively. We defined the "physiologic watershed" as a region where CBF was below the 10$^{th}$ percentile of mean WM CBF in a young healthy cohort. We conducted linear regression to evaluate the relationship between CBF and OEF with structural and microstructural WM injury defined by FLAIR WMH and DTI, respectively. We conducted ANOVA to determine if OEF was increased in proximity to WMH lesions.

**Results:** In a cohort of 42 participants (age 50–80), the physiologic watershed region spatially overlapped with regions of highest WMH lesion density. As CBF decreased and OEF increased, WMH density increased. Elevated watershed OEF was associated with greater WMH burden and microstructural disruption, after adjusting for vascular risk factors. In contrast, WM and watershed CBF were not associated with WMH burden or microstructural disruption. Moreover,

**Corresponding Authors:** Peter Kang, MD, MSCI, Washington University School of Medicine, 660 South Euclid Avenue, Campus Box 8111, Saint Louis, Missouri 63110, peterkang@wustl.edu, Telephone: (314) 362-2999, Fax: (314) 362-6033, Jin-Moo Lee, MD, PhD, Washington University School of Medicine, 660 South Euclid Avenue, Campus Box 8111, Saint Louis, Missouri 63110, leejm@wustl.edu, Telephone: (314) 747-1138, Fax: (314) 362-2244.

*First co-authors

†Senior co-authors

Supplemental Materials:
Online Table I–II
Online Figures I–II

OEF progressively increased while CBF decreased, in concentric contours approaching WMH lesions.

**Conclusions:** Chronic hypoxia-ischemia in the watershed region may contribute to CSVD pathogenesis and development of WMH. Watershed OEF may hold promise as an imaging biomarker to identify individuals at risk for CSVD progression.

## Introduction

Dementia is among the most important public health crises globally. Vascular contributions to cognitive impairment and dementia are the second leading cause of dementia after Alzheimer's disease and encompass multiple cerebrovascular pathologies. Neuroimaging endpoints have been used to measure injury due to cerebral small vessel disease (CSVD) and include: white matter hyperintensities (WMH), lacunar strokes, cerebral microbleeds, atrophy, enlarged perivascular spaces and diffusion tensor imaging (DTI) metrics of impaired microstructural integrity.[1] WMH are a valuable imaging biomarker of CSVD because they are easily identified, prevalent, and strongly associated with clinical endpoints including incident stroke, post-stroke outcomes, cognitive impairment and all-cause mortality.[2, 3] Additionally, DTI metrics of impaired microstructural integrity, including low fractional anisotropy (FA) and high mean diffusivity (MD) predict conversion of normal-appearing white matter (NAWM) to WMH.[4, 5]

Although WMH may have multiple etiologies, they are primarily observed with aging and hypertension.[2] While cerebrovascular risk factors have been linked to WMH, much of the variance in WMH remains elusive.[3] Prior studies have suggested a role for chronic hypoperfusion, impaired cerebrovascular reactivity, and blood-brain barrier leakage;[6] however, human studies have yielded conflicting results. Hypertension alters the structure of cerebral blood vessels, leading to atherosclerosis and lipohyalinosis, which in turn may result in chronic hypoperfusion and ischemia.[7] Currently, WMH pathophysiology remains poorly understood and outside a modest effect of blood pressure control,[8] effective preventative strategies are lacking.

Spatial patterns of disease may provide insight into the pathophysiology of CSVD. Notably, WMH have a predilection for the periventricular and deep white matter (WM), a region overlapping with the cerebral internal borderzone.[9] Prior work suggests that regions of nadir cerebral blood flow (CBF) may be vulnerable to WMH.[10] While the internal borderzone is defined anatomically, a watershed region defined by perfusion has not been described.

In this study, we measured CBF to delineate a physiologic watershed. Further, we studied regional CBF and oxygen extraction fraction (OEF) in patients with CSVD, focusing on the WM and physiologic watershed regions. We hypothesized that the watershed region would have the highest density of WMH and impaired microstructural integrity, and would be associated with the highest elevation of OEF. We further hypothesized that NAWM surrounding WMH would demonstrate elevated OEF, suggesting hypoxia-ischemia may precede WMH development.

## Materials and Methods

### Data are available upon request.

**Study Design and Participants—**This study was approved by the Institutional Review Board at the Washington University School of Medicine. Informed consent was obtained for all participants. Participants aged 50–80 years old with and without cerebrovascular risk factors (lacunar stroke, hypertension, diabetes mellitus, and hyperlipidemia) were recruited at the Washington University Medical Center in St. Louis, Missouri between 2016 and 2019. Exclusion criteria included any reported or known history of genetic CSVDs, intracranial mass, Alzheimer's dementia, probable cerebral amyloid angiopathy (defined by the modified Boston criteria),[11] intracranial atherosclerotic disease (defined with a pre-existing clinical diagnosis, history of large vessel stroke or greater than 70% stenosis of the intracranial arteries on vascular imaging), atrial fibrillation, ischemic stroke caused by a large vessel occlusion, or contraindications to MRI. We also excluded participants with a neurologic history other than stroke or transient ischemic attack or who were pregnant.

**Imaging Protocol and Processing—**Participants underwent brain MRI on a Siemens 3T Tim Trio, 3T Biograph mMR, or 3T MAGNETOM PrismaFit scanner (Siemens Healthineer, Erlangen, Germany). Standard three-dimensional MP-RAGE (magnetization prepared rapid acquisition gradient echo) T1 (echo time/repetition time [TE/TR] = 2.86/1800 ms; inversion time [TI] = 1000 ms; flip angle = 8 degrees; acquired voxel resolution 1×1×1 mm, 0.48×0.48×1 mm voxel resolution after in-plane interpolation), fluid attenuated inversion recovery (FLAIR, TE/TR 93/9000 ms; TI, 2500 ms; 0.86×0.86 mm in-plane resolution, 3-mm slice thickness), and magnetic resonance angiography sequences were acquired. A board certified neurologist (P.K.) manually delineated WMH on the FLAIR images using Medical Image Processing, Analysis, and Visualization software (https://mipav.cit.nih.gov). To account for variation in brain volume, we normalized WMH to whole brain volume. We identified lacunar infarcts on FLAIR imaging and cerebral microhemorrhages or cortical superficial siderosis on susceptibility weighted imaging sequences. Magnetic resonance angiography was available in 36 of 42 participants to evaluate for stenosis of the intracranial arteries > 70%, which was absent in all cases.

**CBF and OEF Imaging Parameters—**Participants underwent MRI with a 2D multi-slice pseudocontinuous arterial spin labeling (pCASL) sequence to measure CBF with the following parameters: TE/TR 12/3780 ms; in-plane voxel resolution 3×3 mm; slice thickness of 5 mm, 22 slices; 40 label and control pairs; a labeling duration of 2 s, a post-labeling delay (PLD) of 1.5 s (range 1.5 to 2.45 s for the inferior to superior slices).[12] Blood T1 was measured individually in the superior sagittal sinus with an inversion-recovery echo planar imaging sequence.[13] We utilized an asymmetric spin echo (ASE) sequence to measure OEF on a voxel-wise and region of interest (ROI) basis with the following parameters: TE1/TE2/TR 60.4/94.6/4740 ms, in-plane voxel resolution 1.72×1.72 mm after in-plane interpolation; slice thickness of 3 mm, 26 slices.[14] Quantification of CBF and OEF have been described previously.[14, 15] For regional CBF and OEF measurements inside ROIs, individual mean CBF and OEF values within those regions were calculated. In order to

account for inter-subject variation in whole brain OEF, mean WM and watershed regional OEF values were normalized as a ratio to whole brain OEF.

**DTI Protocol and Processing—**DTI was acquired using an echo planar imaging sequence. A DTI scan with 25 non-collinear diffusion directions and a maximal b value of 1400 s/mm$^2$ was performed in 37 out of 42 participants with TE/TR=85/10600 ms, and in 4 participants with TE/TR=75/4500 ms (with multi-band excitation). One subject was scanned using a 12 non-collinear diffusion directions with a maximal b value of 1000 s/mm$^2$ and TE/TR=83/12200 ms. The voxel resolution was 2×2× 2 mm$^3$. We reconstructed the diffusion tensor in each voxel from the DTI signal. The diffusion tensor maps including FA and MD were derived using the diffusion toolbox by FSL (Oxford University, UK).

**Image Segmentation and Registration—**Individual MP-RAGE images were segmented into gray matter (GM), WM and cerebrospinal fluid probability maps using Statistical Parametric Mapping (SPM12).[16] The GM mask was defined as voxels with highest probability of GM, and the WM mask was defined as voxels with highest probability of WM. Voxels with a probability less than 0.9 of being classified as GM or WM or those that were cerebrospinal fluid were removed from masks. All manually outlined WMH voxels were considered WM to correct for possible misclassification of T1 hypointense WMH voxels as GM. FMRIB's Linear Image registration Tool co-registered images obtained within a scanning session.[17] All images and maps were then co-registered to the International Consortium for Brain Mapping atlas using Advanced Normalization Tools for non-linear registration.[18] We visually inspected the images to confirm accurate alignment across all maps. We did not remove WMH lesions from white matter or watershed ROIs, as this would have resulted in different ROIs for each participant, potentially heightening any differences in physiologic parameters due to differing spatial regions.

**NAWM ROI for DTI Analyses—**A WMH lesion density map was calculated across all subjects. Because of the intrinsic spatial variation in DTI measurements [19], we used a common ROI amongst all cases which included all WM voxels that were categorized as NAWM in ≥ 95% of aggregated voxels. This common NAWM ROI was used for all DTI analyses.

**Defining the Watershed Region—**Currently, there are no standardized means to quantitatively define the watershed region.[10] To this end, we created average CBF maps from a group of 32 healthy young participants without vascular risk factors (age ≤ 55) and delineated tiers of blood flow as a percentile of average WM CBF to define the nadir of WM perfusion. This included eight healthy participants from the present study as well as a separate cohort of normal healthy volunteers with a goal to physiologically define a watershed region without the confounders of aging and CSVD (Supplementary Table I). Supplementary Figure I demonstrates three contours of WM CBF representing the three lowest deciles. The lowest decile is located in the deep WM and approximates anatomic descriptions of the internal borderzone.[20] We henceforth refer to this ROI as the "physiological watershed."

### Statistical Analysis

Normality of the data was evaluated by visual inspection and the Shapiro-Wilks test of normality. Data are described as median (interquartile range) or frequency (%). Correlations were performed using the Spearman's rank correlation coefficient. To evaluate the independent effects of WM and watershed CBF and OEF on WMH volume and DTI FA and MD, multivariate linear regression with a stepwise model of predictor variable entry was utilized. In addition to regional CBF and OEF, we evaluated the effect of age, sex, race, type 2 diabetes, hypertension and hyperlipidemia on the outcomes for possible entry into these models. These variables were assessed with a questionnaire by research staff. A univariate $p<0.2$ was required for entry into the model and $p<0.05$ for retention. Model diagnostics were evaluated to assess for multicollinearity (variance inflation factor > 5). None of the models raised concerns for multicollinearity. Unstandardized residuals were evaluated visually and with the Shapiro-Wilks test to assess whether they fit a Gaussian distribution. Regional comparison within individual subjects were performed with a repeated measures ANOVA using the Greenhouse-Geisser correction if sphericity was violated. Post-hoc comparison of these main effects was performed with the Bonferroni adjustment for multiple comparisons.

## Results

### Cohort Characteristics

Forty-two participants were included in this study. Participant characteristics are listed in Table 1. One participant did not undergo pCASL. The median WMH volume was 8.35 $cm^3$ and the median WMH volume to whole brain ratio was 0.0081. Six participants had no WMH. Few participants had lacunes (14.3%) or cerebral microbleeds (15%) and none had cortical superficial siderosis.

### Watershed OEF is Associated with WMH volume

To examine the relationship between hemodynamic and oxygen metabolic stress and WMH burden, we quantified the association of CBF and OEF with WMH volume (Figure 1). While WM and watershed OEF were correlated with WMH burden, WM and watershed CBF were not. Next, we performed multivariate linear regression to determine the independent influence of WM and watershed OEF on WMH volume (Table 2). Although there is spatial overlap between WM and watershed OEF, we allowed them both to be entered into the models to determine if one was a more potent predictor. On univariate analysis, age, hypertension, diabetes mellitus, and hyperlipidemia met criteria for inclusion into the multivariate model. Of these, only hypertension and watershed OEF were independent predictors of WMH volume, accounting for almost 70% of the variance in WMH volume ($R^2_{adj}$ 0.697). WM OEF was not retained in the model.

### Watershed OEF is Associated with Impaired Microstructural Integrity

Prior work has shown that a decline in WM microstructural integrity, measured by DTI, precedes WMH development, suggesting that DTI change may be a precursor to WMH in CSVD.[4, 5] To examine the relationship between hemodynamic and oxygen metabolic stress

and microstructural disruption, we quantified the association of CBF and OEF with DTI FA and MD in the common NAWM ROI. While WM ($\rho$ = −0.431, p = 0.004) and watershed OEF were correlated with FA, WM ($\rho$ = 0.046, p = 0.776) and watershed CBF were not. Similarly, while WM ($\rho$ = 0.504, p = 0.001) and watershed OEF were correlated with MD, WM ($\rho$ = −0.193, p = 0.227) and watershed CBF were not (Figure 2, WM not shown).

Next, we performed multivariate linear regression to determine the independent influence of WM and watershed OEF on FA as well as WM and watershed OEF and watershed CBF on MD (Table 2). Watershed CBF was included for entry into the MD model because it met the threshold of $p < 0.2$. On univariate analysis, hypertension, diabetes mellitus, race and sex met criteria for inclusion into the multivariate model for FA. Of these, watershed OEF and diabetes were independent predictors of FA. Watershed OEF contributed to most of the variance ($R^2_{adj}$ = 0.245), and diabetes increased the $R^2_{adj}$ to 0.303. On univariate analysis, age, hypertension, diabetes mellitus and sex met criteria for inclusion into the multivariate model for MD. Of these, only hypertension and watershed OEF were independent predictors of MD. While hypertension contributed to most of the variance ($R^2_{adj}$ = 0.358), watershed OEF increased the $R^2_{adj}$ to 0.423. While watershed OEF was independently associated with FA and MD in these models, WM OEF was not. None of the variables were determined to be multicollinear (see Supplementary Table II).

## The Watershed Demonstrates Low CBF, High OEF and Overlaps with WMH Topology

To investigate the spatial relationship between CBF, OEF, and WMH, we overlaid the watershed ROI onto average CBF, OEF, and WMH density maps (Figure 3 A–C). Visual inspection demonstrated that the watershed ROI had striking overlap with the regions of lowest CBF and highest OEF. Moreover, this watershed ROI derived from healthy young participants overlapped with regions of highest WMH density in our cohort. We found an inverse relationship between average CBF and OEF (Figure 3D) when spatially aggregating voxels by OEF. We then examined CBF and OEF by aggregated voxels of WMH density. Using averaged maps, pooled voxels with lower CBF and higher OEF had a higher incidence of WMH (Figure 3E).

## Hypoxic-Ischemic Physiology at the Leading Edge of WMH Growth

Previous work has shown that decreased CBF and DTI measures of impaired microstructural integrity in NAWM surrounding WMH lesions predicts expansion of WMH, suggesting the importance of altered blood flow in the CSVD.[5, 21] To further understand the role hypoxic-ischemic physiology in the pathogenesis of WMH, we measured CBF and OEF inside lesions and in concentric NAWM ROIs, 0–4mm and 4–8mm outward (Figure 4). CBF declined in contours approaching the lesions. Moreover, OEF increased in contours approaching WMH and was highest within the lesion. Similar to previous work by other investigators, we found a trend towards lower FA and significantly higher MD at the leading edge of WMH growth (Supplementary Figure II), suggesting the presence of impaired microstructural integrity before lesions are visible on FLAIR.[4, 5, 21]

## Discussion

In this prospective study, we demonstrated that the physiologic watershed region is particularly vulnerable to the development of WMH. Defining the physiologic watershed as the lowest 10$^{th}$ percentile of mean WM CBF in a young healthy group, we found that this region had remarkable spatial overlap with WMH lesion density in our older cohort. Our data demonstrate that OEF is selectively elevated in the physiological watershed and correlates with both WMH burden and loss of microstructural integrity in NAWM. Notably, watershed OEF was preferentially retained in the multivariate models over WM OEF, suggesting that oxygen metabolic stress in the watershed is a better predictor of WM injury compared to metabolic stress in a broader WM region. This regional elevation of OEF is indicative of an oxygen supply-demand deficit, implicating hypoxia-ischemia in CSVD pathogenesis. While CBF did not predict CSVD endpoints, we found that low CBF regions co-localized with high OEF regions and that low CBF and high OEF followed areas of higher WMH density. Furthermore, we found OEF progressively increased and CBF decreased in concentric contours surrounding WMH, suggesting that hypoxic-ischemic conditions exist at the leading edge of lesion progression.

Our study findings are consistent with a prior studies investigating oxygen metabolism in CSVD. Previous work[22] found increased OEF and decreased CBF in the centrum semiovale using positron emission tomography (PET). This large WM ROI, necessitated by the lower spatial resolution of PET, encompasses our physiologic watershed ROI. Indeed, these early PET studies were unable to resolve the watershed region or concentric contours that we examined using MRI.

In the current study, we defined the watershed as a nadir in perfusion—a more quantitative physiological definition compared to the classic anatomic description.[23] The deep WM region delineated by the lowest perfusion circumscribes a region with the lowest density of penetrating arterioles and approximates the internal borderzone.[23] Natural variation in watershed vulnerability is observed in different strains of mice, which demonstrate strain-dependent vulnerability to experimental stroke with middle cerebral artery occlusion.[24] Indeed, this variation in ischemic vulnerability has revealed genetic contributions to the development of watershed collateral vessels, which develop with distinct mechanisms from arterial angiogenesis.[25] Importantly, these collateral vessels are particularly sensitive to aging and vascular risk factors.[25] This may, in part, explain the intrinsic variability in human CSVD risk beyond the presence of vascular risk factors. Indeed we found that watershed OEF independently explains the variance in WMH burden above that of just hypertension alone.

Elevated watershed OEF was strongly associated with lower FA and higher MD in the NAWM of this cohort—signatures of disrupted microstructural integrity—indicating that individuals with higher levels of hypoxic-ischemic stress may be at increased risk of developing WMH. In our cohort, watershed OEF demonstrated the highest $R^2_{adj}$ in FA, even more than diabetes. Hypertension provided the majority of the variance explained in MD, but notably, watershed OEF added significantly to this model.

Prior work has shown that NAWM regions surrounding lesions which eventually convert to WMH have significantly higher MD and lower FA than regions that do not, reflecting early injury to WM microstructure before radiographic lesions are present (Supplementary Figure II).[4, 5] Importantly, we found that in addition to decreased CBF, there is increased OEF in tissue surrounding WMH lesions, suggesting that active hypoxia-ischemia is present in proximity to WMH progression. Our finding that OEF is highest inside the lesion suggests that WMH lesions may include areas of metabolically active but highly stressed tissue, rather than uniformly infarcted tissue. Indeed, previous histopathologic evaluations of WMH have shown mixed findings along the spectrum of disease, [26] and others have suggested that heterogeneity of tissue viability may be reflected in T1 signal heterogeneity within WMH.[2]

OEF may provide a more robust biomarker of viable tissue “at risk” for infarction due to several challenges in interpreting low CBF measurements. Previous work has shown decreased CBF in proximity to WMH lesions [5, 21], but concurrent OEF measurements are required to determine whether hypoxia-ischemia is present. Low CBF may be attributable to two distinct underlying mechanisms: 1) a matched low oxygen supply and demand as seen in Alzheimer’s disease (atrophy) or following ischemic stroke (infarction);[27, 28] 2) mismatched oxygen supply and demand (low CBF and elevated OEF, signifying hypoxia-ischemia) as seen in misery perfusion of ischemic tissue. Thus, OEF measures are important for interpreting the meaning of low CBF. Another confounding issue with understanding low CBF in CSVD, is its spatial heterogeneity. CBF is more than twice as high in GM compared to WM.[29] Moreover, even within the WM, it is heterogeneous and reaches a nadir within the watershed region (Supplementary Figure I). Because WMH have a spatial propensity for the watershed region, mean CBF values will be lower in WMH compared to NAWM simply by virtue of their superimposed location. In contrast, OEF is relatively homogenous in its spatial distribution, with similar values in GM and WM.[30] This relative homogeneity of OEF permits the comparison of OEF values across space.

Although we found that watershed OEF was influential on CSVD endpoints (WMH and disrupted microstructural integrity), WM and watershed CBF were not. It is possible that we were unable to detect a relationship between CBF and WMH volume due to a potential technical floor effect of pCASL in deep WM regions, where the signal to noise ratio is unfavorable.[31] Furthermore, intra-subject repeatability of arterial spin labeling measurements of perfusion in cerebrovascular disease is unclear and a small CBF difference cannot be detected due to the large test-retest CBF measurement variability.[32] This may be heightened in the physiologic watershed where perfusion is lowest. However, it is also possible that single CBF measures do not accurately capture the dynamics of perfusion in CSVD. For example, CBF fluctuates over time in the healthy brain in response to autoregulation and neurovascular coupling to meet moment-to-moment changes in oxygen metabolic demand [33]. Prior work has implicated impaired cerebrovascular reactivity in CVSD [34] which may lead to episodic mismatch between oxygen demand and supply, resulting in intermittent hypoxia-ischemia. Thus, OEF may provide a more informative marker of hypoxia-ischemia than CBF.

As a whole, prior work regarding regional CBF in CSVD lacks consensus.[22, 35] While several studies have shown decreased resting CBF in CSVD patients with WMH; methods

were variable, and studies often did not use age-matched controls. [3, 21, 35] Further, resting CBF is known to decrease with age even in the absence of vascular risk factors [3]. A meta-analysis of CSVD cohorts found that the relationship between low CBF and WMH burden was weakened after removing non-age-matched and demented subjects, suggesting that differences in CBF observed in CSVD may be attributable to age or dementia.[1] A large longitudinal study found no relationship between WM CBF and WMH volume, nor WM CBF and WMH growth over 5 years.[36] Another study found that baseline CBF was not related to WMH progression over time, but rather, baseline WMH volume predicted a longitudinal decline in CBF.[37]

Strengths of this study include measurement of voxel-wise OEF in a population with a range cerebrovascular risk factors and WMH volumes. Further, we examined the voxel-wise spatial relationship between CBF, OEF, and WMH in a CSVD cohort, allowing for a more complete understanding of ischemic vulnerability in CSVD. However, there are several limitations. Firstly, the cross-sectional study design limits the ability to establish a temporal relationship between regional OEF elevation and the conversion of NAWM into new lesions. We will be performing longitudinal studies to examine whether OEF predicts CSVD progression. In addition, this work was done on a small cohort and future work will use larger sample sizes to test these hypotheses. Because our CSVD group is an aged population, it is possible that our cohort has mixed pathologies, although we excluded participants with any known history of Alzheimer dementia. It is possible that we were unable to demonstrate significance with CBF in the WM and watershed region due to a technical floor effects of pCASL in deep WM regions (as discussed above). A PLD shorter than the arterial transit time leads to an underestimation of CBF. In our study, the actual PLD ranged from 1.5 s to 2.45 s for the inferior to the superior slices with an ascending slice acquisition order. Since the watershed region was part of the superior two thirds of the slices, the effective PLD ranged from 1.8 s to 2.45 s. Therefore, CBF may be underestimated in regions encompassed in the WM and watershed ROIs. It is possible that the watershed may be more affected by this relative to the WM ROI. Finally, the majority (36 of 42) but not all participants had vascular imaging to definitively rule out intracranial atherosclerotic disease.

## Summary/Conclusions

In conclusion, we describe a physiologically-defined watershed, delineated by a quantitative nadir in CBF, and implicate chronic watershed hypoxia-ischemia in the development and progression of CSVD. We demonstrate the importance of regional measures of OEF, rather than CBF, in WMH and early WM injury in individuals with CSVD. Future work will longitudinally examine regional elevations in OEF as predictors of progression in WMH and impaired microstructural integrity in CSVD and vascular contributions to cognitive impairment and dementia.

## Supplementary Material

Refer to Web version on PubMed Central for supplementary material.

## Sources of Funding:

Research reported in this publication was supported by the National Center for Advancing Translational Sciences of the NIH under Award Number KL2 TR002346. The content is solely the responsibility of the authors and does not necessarily represent the official views of the NIH (P.K.). American Academy of Neurology Clinical Research Training Scholarship (P.K.), NIH R01HL129241 (A.L.F) NIH 1R011NS082561 (H.A.), NIH 1P30NS098577 (Imaging Core, H.A.), NIH RF1NS116565 (H.A. and A.L.F), NIH R01NS085419, U24 NS107230 (J.M.L).

**Conflict(s)-of-Interest/Disclosure(s):** Dr. Lee reports grants from Biogen.

## Non-Standard Abbreviations and Acronyms

| | |
|---|---|
| **CSVD** | cerebral small vessel disease |
| **WMH** | white matter hyperintensities |
| **DTI** | diffusion tensor imaging |
| **FA** | fractional anisotropy |
| **MD** | mean diffusivity |
| **NAWM** | normal appearing white matter |
| **WM** | white matter |
| **CBF** | cerebral blood flow |
| **OEF** | oxygen extraction fraction |
| **pCASL** | pseudocontinuous arterial spin labeling |
| **PLD** | post-labeling delay |
| **ASE** | asymmetric spin echo |
| **ROI** | region of interest |
| **GM** | gray matter |
| **PET** | positron emission tomography |

## References

1. Shi Y, Thrippleton MJ, Makin SD, Marshall I, Geerlings MI, de Craen AJM, van Buchem MA and Wardlaw JM. Cerebral blood flow in small vessel disease: A systematic review and meta-analysis. J Cereb Blood Flow Metab. 2016;36:1653–1667. [PubMed: 27496552]
2. Wardlaw JM, Valdes Hernandez MC and Munoz-Maniega S. What are white matter hyperintensities made of? Relevance to vascular cognitive impairment. J Am Heart Assoc. 2015;4:001140. [PubMed: 26104658]
3. Wardlaw JM William M Feinberg Award for Excellence in Clinical Stroke: Small Vessel Disease; a Big Problem, But Fixable. Stroke. 2018;49:1770–1775. [PubMed: 29895535]
4. van Leijsen EMC, Bergkamp MI, van Uden IWM, Ghafoorian M, van der Holst HM, Norris DG, Platel B, Tuladhar AM and de Leeuw FE. Progression of White Matter Hyperintensities Preceded by Heterogeneous Decline of Microstructural Integrity. Stroke. 2018;49:1386–1393. [PubMed: 29724890]

5. Promjunyakul NO, Dodge HH, Lahna D, Boespflug EL, Kaye JA, Rooney WD and Silbert LC. Baseline NAWM structural integrity and CBF predict periventricular WMH expansion over time. Neurology. 2018;90:e2119–e2126. [PubMed: 29769375]
6. Joutel A and Chabriat H. Pathogenesis of white matter changes in cerebral small vessel diseases: beyond vessel-intrinsic mechanisms. Clin Sci (Lond). 2017;131:635–651. [PubMed: 28351960]
7. Iadecola C and Davisson RL. Hypertension and cerebrovascular dysfunction. Cell Metab. 2008;7:476–84. [PubMed: 18522829]
8. Dufouil C, Chalmers J, Coskun O, Besancon V, Bousser MG, Guillon P, MacMahon S, Mazoyer B, Neal B, Woodward M, Tzourio-Mazoyer N, Tzourio C and Investigators PMS. Effects of blood pressure lowering on cerebral white matter hyperintensities in patients with stroke: the PROGRESS (Perindopril Protection Against Recurrent Stroke Study) Magnetic Resonance Imaging Substudy. Circulation. 2005;112:1644–50. [PubMed: 16145004]
9. Rostrup E, Gouw AA, Vrenken H, van Straaten EC, Ropele S, Pantoni L, Inzitari D, Barkhof F and Waldemar G. The spatial distribution of age-related white matter changes as a function of vascular risk factors--results from the LADIS study. Neuroimage. 2012;60:1597–607. [PubMed: 22305990]
10. Dolui S, Tisdall D, Vidorreta M, Jacobs DR Jr., Nasrallah IM, Bryan RN, Wolk DA and Detre JA. Characterizing a perfusion-based periventricular small vessel region of interest. Neuroimage Clin. 2019;23:101897. [PubMed: 31233954]
11. Greenberg SM and Charidimou A. Diagnosis of Cerebral Amyloid Angiopathy: Evolution of the Boston Criteria. Stroke. 2018;49:491–497. [PubMed: 29335334]
12. Dai W, Garcia D, de Bazelaire C and Alsop DC. Continuous flow-driven inversion for arterial spin labeling using pulsed radio frequency and gradient fields. Magn Reson Med. 2008;60:1488–97. [PubMed: 19025913]
13. Eldeniz C, Finsterbusch J, Lin W and An H. TOWERS: T-One with Enhanced Robustness and Speed. Magn Reson Med. 2016;76:118–26. [PubMed: 26228530]
14. An H and Lin W. Impact of intravascular signal on quantitative measures of cerebral oxygen extraction and blood volume under normo- and hypercapnic conditions using an asymmetric spin echo approach. Magn Reson Med. 2003;50:708–16. [PubMed: 14523956]
15. Guilliams KP, Fields ME, Ragan DK, Eldeniz C, Binkley MM, Chen Y, Comiskey LS, Doctor A, Hulbert ML, Shimony JS, Vo KD, McKinstry RC, An H, Lee JM and Ford AL. Red cell exchange transfusions lower cerebral blood flow and oxygen extraction fraction in pediatric sickle cell anemia. Blood. 2018;131:1012–1021. [PubMed: 29255068]
16. Ashburner J and Friston KJ. Unified segmentation. Neuroimage. 2005;26:839–51. [PubMed: 15955494]
17. Jenkinson M, Bannister P, Brady M and Smith S. Improved optimization for the robust and accurate linear registration and motion correction of brain images. Neuroimage. 2002;17:825–41. [PubMed: 12377157]
18. Fonov VSE,AC; McKinstry RC; Almli CR; Collins DL Unbiased nonlinear average age-appropriate brain templates from birth to adulthood. Neuroimage. 2009;47:Page S102.
19. Sullivan EV, Rohlfing T and Pfefferbaum A. Quantitative fiber tracking of lateral and interhemispheric white matter systems in normal aging: relations to timed performance. Neurobiol Aging. 2010;31:464–81. [PubMed: 18495300]
20. Mangla R, Kolar B, Almast J and Ekholm SE. Border zone infarcts: pathophysiologic and imaging characteristics. Radiographics. 2011;31:1201–14. [PubMed: 21918038]
21. Promjunyakul NO, Lahna DL, Kaye JA, Dodge HH, Erten-Lyons D, Rooney WD and Silbert LC. Comparison of cerebral blood flow and structural penumbras in relation to white matter hyperintensities: A multi-modal magnetic resonance imaging study. J Cereb Blood Flow Metab. 2016;36:1528–36. [PubMed: 27270266]
22. Nezu T, Yokota C, Uehara T, Yamauchi M, Fukushima K, Toyoda K, Matsumoto M, Iida H and Minematsu K. Preserved acetazolamide reactivity in lacunar patients with severe white-matter lesions: 15O-labeled gas and H2O positron emission tomography studies. J Cereb Blood Flow Metab. 2012;32:844–50. [PubMed: 22252236]
23. Momjian-Mayor I and Baron JC. The pathophysiology of watershed infarction in internal carotid artery disease: review of cerebral perfusion studies. Stroke. 2005;36:567–77. [PubMed: 15692123]

24. Prabhakar P, Zhang H, Chen D and Faber JE. Genetic variation in retinal vascular patterning predicts variation in pial collateral extent and stroke severity. Angiogenesis. 2015;18:97–114. [PubMed: 25369734]
25. Faber JE, Zhang H, Lassance-Soares RM, Prabhakar P, Najafi AH, Burnett MS and Epstein SE. Aging causes collateral rarefaction and increased severity of ischemic injury in multiple tissues. Arterioscler Thromb Vasc Biol. 2011;31:1748–56. [PubMed: 21617137]
26. Munoz DG, Hastak SM, Harper B, Lee D and Hachinski VC. Pathologic correlates of increased signals of the centrum ovale on magnetic resonance imaging. Arch Neurol. 1993;50:492–7. [PubMed: 8489405]
27. Yamaji S, Ishii K, Sasaki M, Imamura T, Kitagaki H, Sakamoto S and Mori E. Changes in cerebral blood flow and oxygen metabolism related to magnetic resonance imaging white matter hyperintensities in Alzheimer's disease. J Nucl Med. 1997;38:1471–4. [PubMed: 9293811]
28. Sette G, Baron JC, Mazoyer B, Levasseur M, Pappata S and Crouzel C. Local brain haemodynamics and oxygen metabolism in cerebrovascular disease. Positron emission tomography. Brain. 1989;112 ( Pt 4):931–51. [PubMed: 2789086]
29. Parkes LM, Rashid W, Chard DT and Tofts PS. Normal cerebral perfusion measurements using arterial spin labeling: reproducibility, stability, and age and gender effects. Magn Reson Med. 2004;51:736–43. [PubMed: 15065246]
30. Ibaraki M, Miura S, Shimosegawa E, Sugawara S, Mizuta T, Ishikawa A and Amano M. Quantification of cerebral blood flow and oxygen metabolism with 3-dimensional PET and 15O: validation by comparison with 2-dimensional PET. J Nucl Med. 2008;49:50–9. [PubMed: 18077532]
31. van Gelderen P, de Zwart JA and Duyn JH. Pittfalls of MRI measurement of white matter perfusion based on arterial spin labeling. Magn Reson Med. 2008;59:788–95. [PubMed: 18383289]
32. Wu B, Lou X, Wu X and Ma L. Intra- and interscanner reliability and reproducibility of 3D whole-brain pseudo-continuous arterial spin-labeling MR perfusion at 3T. J Magn Reson Imaging. 2014;39:402–9. [PubMed: 23723043]
33. Fox MD and Raichle ME. Spontaneous fluctuations in brain activity observed with functional magnetic resonance imaging. Nat Rev Neurosci. 2007;8:700–11. [PubMed: 17704812]
34. Sam K, Crawley AP, Conklin J, Poublanc J, Sobczyk O, Mandell DM, Venkatraghavan L, Duffin J, Fisher JA, Black SE and Mikulis DJ. Development of White Matter Hyperintensity Is Preceded by Reduced Cerebrovascular Reactivity. Ann Neurol. 2016;80:277–85. [PubMed: 27352039]
35. Hatazawa J, Shimosegawa E, Satoh T, Toyoshima H and Okudera T. Subcortical hypoperfusion associated with asymptomatic white matter lesions on magnetic resonance imaging. Stroke. 1997;28:1944–7. [PubMed: 9341700]
36. Nylander R, Fahlstrom M, Rostrup E, Kullberg J, Damangir S, Ahlstrom H, Lind L and Larsson EM. Quantitative and qualitative MRI evaluation of cerebral small vessel disease in an elderly population: a longitudinal study. Acta Radiol. 2018;59:612–618. [PubMed: 28814098]
37. van der Veen PH, Muller M, Vincken KL, Hendrikse J, Mali WP, van der Graaf Y, Geerlings MI and Group SS. Longitudinal relationship between cerebral small-vessel disease and cerebral blood flow: the second manifestations of arterial disease-magnetic resonance study. Stroke. 2015;46:1233–8. [PubMed: 25804924]

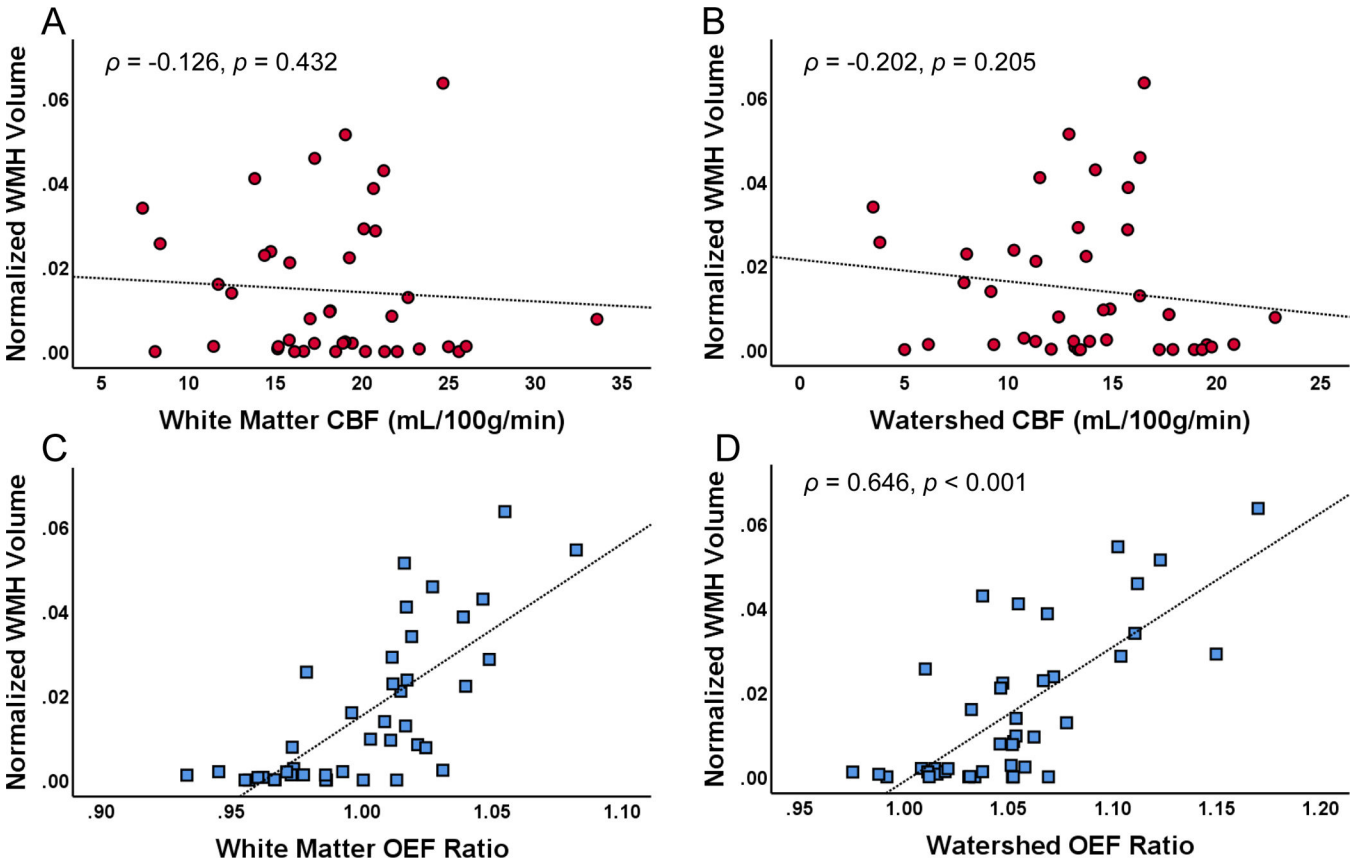


**Figure 1. Watershed oxygen extraction fraction (OEF) is associated with white matter hyperintensity (WMH) volume.**

**(A)** White matter and **(B)** watershed cerebral blood flow (CBF) were not associated with WMH volume. In contrast, **(C)** white matter and **(D)** watershed OEF ratio correlated with WMH volume.

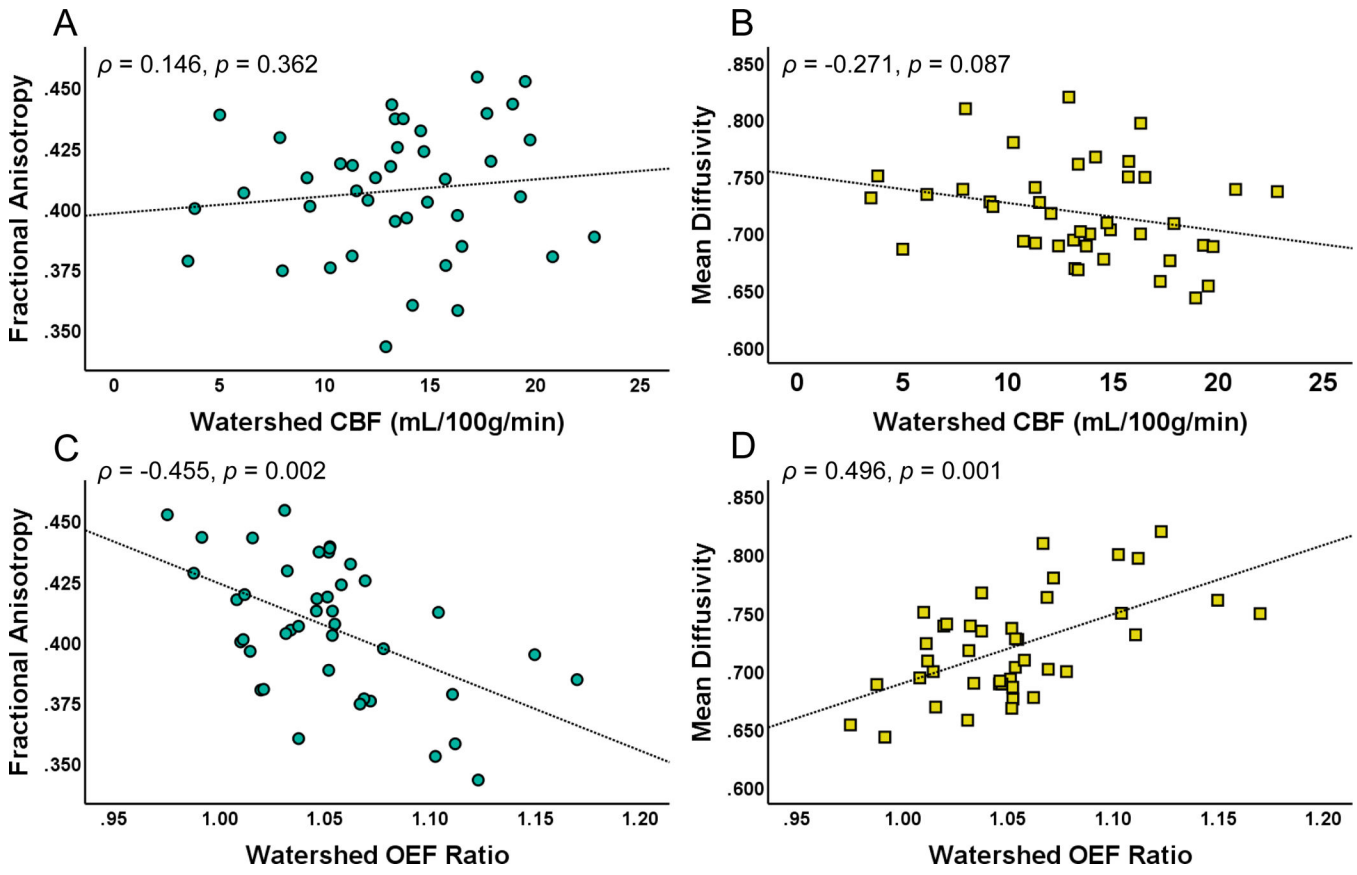


**Figure 2. Watershed oxygen extraction fraction (OEF) is associated with loss of microstructural integrity.**

Watershed cerebral blood flow (CBF) was not associated with **(A)** fractional anisotropy (FA) or **(B)** mean diffusivity (MD) in a common normal-appearing white matter region. However, elevated watershed oxygen extraction fraction (OEF) ratio was associated with **(C)** decreased FA and **(D)** elevated MD.

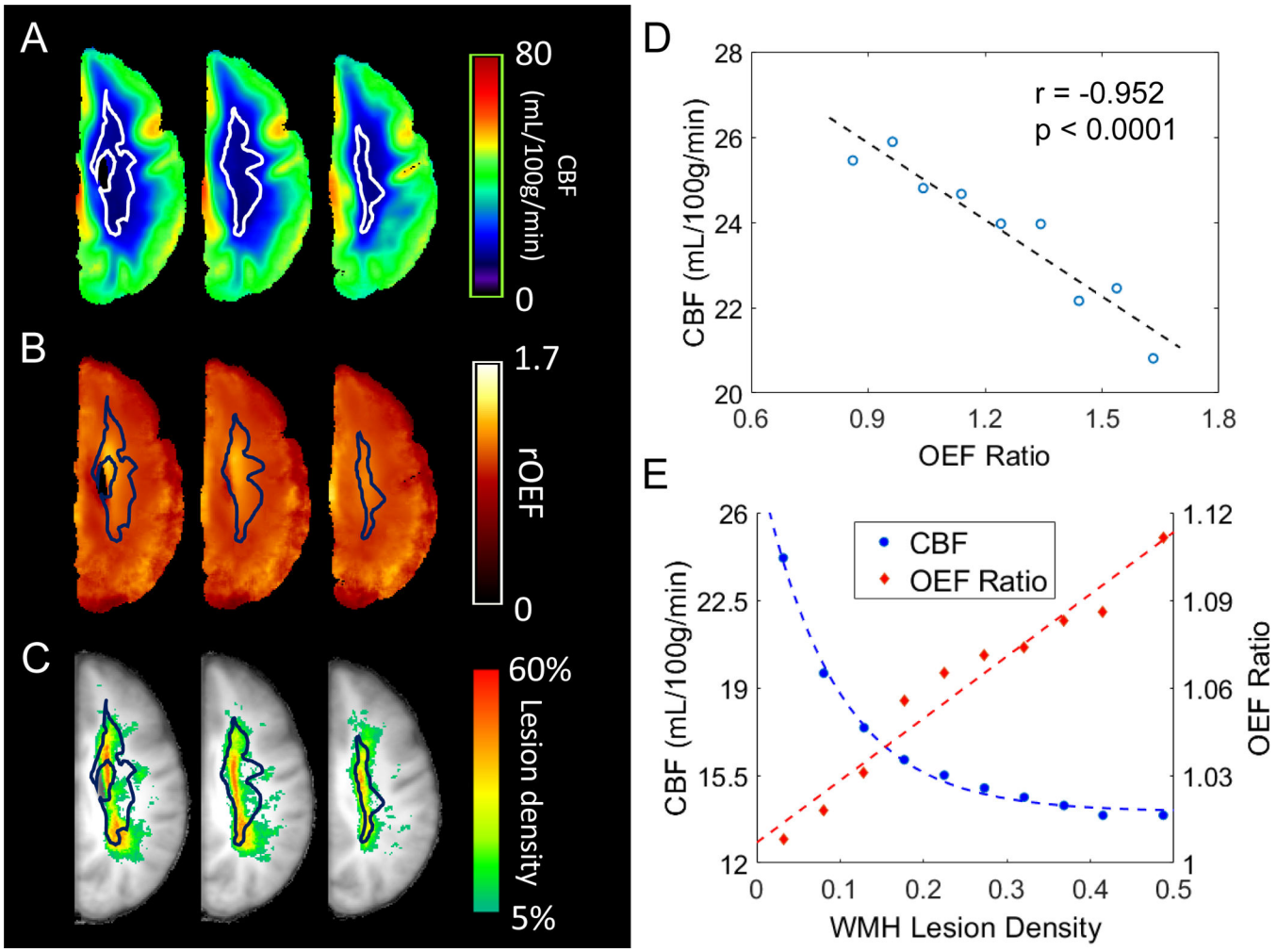


**Figure 3. White matter hyperintensities (WMH) cluster in the physiologic watershed.**

Average cerebral blood flow (CBF) map (A), average oxygen extraction fraction (OEF) ratio map (B), and WMH lesion density map (C) were calculated from all 42 subjects. The watershed (outlined, panels A-C), delineated by the lowest 10$^{th}$ percentile CBF in a young healthy cohort (Supplementary Figure I)has remarkable overlap with the CBF nadir **(A)**, the region of highest OEF elevation **(B)** and the highest density of WMH in the older study cohort **(C).** White matter voxels with group average OEF ranging from 0.8 to 1.6 were grouped into 8 bins with an increment of 0.1 and a final bin of OEF>1.6. Average CBF and OEF were obtained from these grouped voxels **(D)**. A univariate linear regression demonstrates the inverse spatial association between CBF and OEF. White matter voxels with lesion density ranging from 0–45% were grouped into 9 bins with an increment of 5% as well as a final bin of >45%. Average lesion density, CBF and OEF were obtained from these grouped voxels **(E)**. The relationship between CBF and WMH lesion density is best described by an exponential curve, while OEF and WMH lesion density demonstrate a linear relationship.

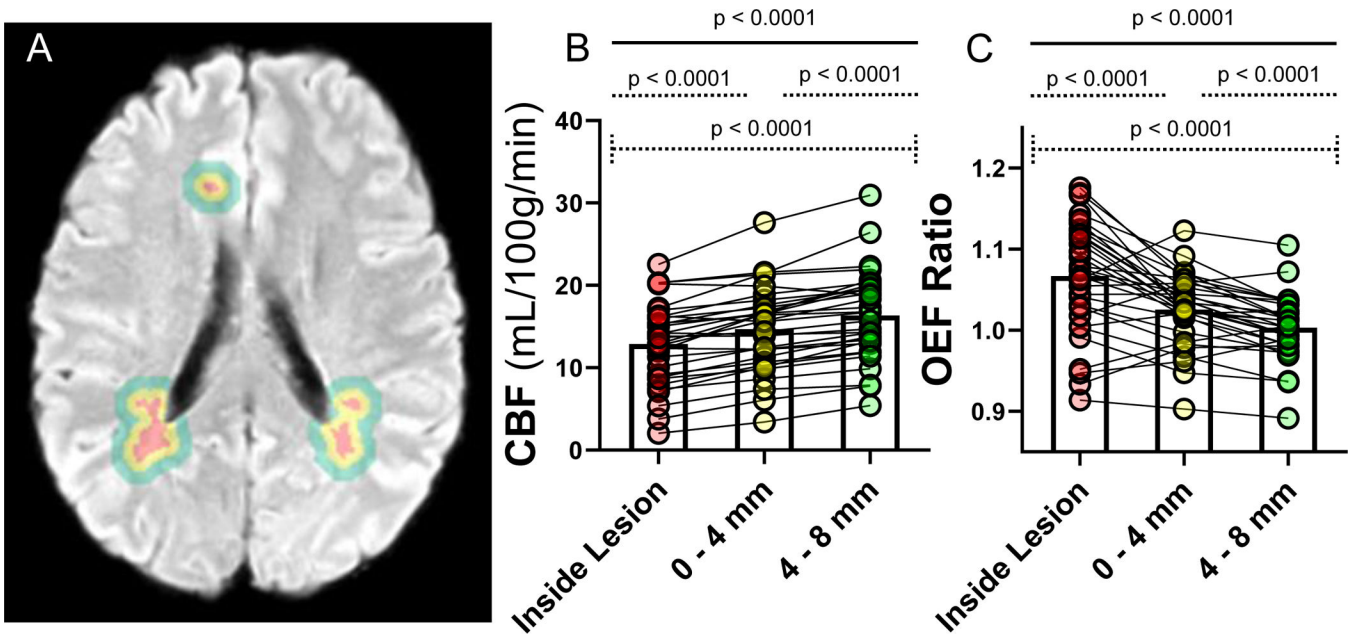


**Figure 4. Cerebral blood flow (CBF) and oxygen extraction fraction (OEF) measurements in concentric contours surrounding lesions suggest hypoxia-ischemia in proximity to white matter hyperintensities (WMH).**

WMH (red) and concentric contours, measuring 0–4 mm (yellow), and 4–8mm (green), surrounding each lesion were generated by dilating the WMH mask in three dimensions for each ROI, excluding cerebrospinal fluid and gray matter. Only participants with >1 cc of WMH were included in this analysis. **(A)**. Comparison of CBF (B) and OEF (C) values across the contours within individuals are shown (spaghetti plots). CBF was lowest inside the lesions and increased with each contour **(B)**. OEF was highest inside the lesions and decreased with each contour **(C)**.

**Table 1.**

Participant Characteristics for the Study Cohort

| | Variables | Study cohort (n=42)* |
|---|---|---|
| Demographics | Age, y, median (IQR) | 65.5 (56.8–73) |
| | Female, n (%) | 20 (47.6) |
| | Black race, n (%) | 30 (71.4) |
| Vascular risk factors | Ischemic stroke, n (%) | 12 (28.6) |
| | Transient ischemic attack, n (%) | 2 (4.8) |
| | Hypertension, n (%) | 19 (45.2) |
| | Diabetes, n (%) | 8 (19) |
| | Hyperlipidemia, n (%) | 8 (19) |
| Imaging characteristics | WMH volume, $cm^3$, median (IQR) | 8.15 (1.04–26.97) |
| | Normalized WMH volume ratio, median (IQR) | 0.0081 (0.0010–0.0263) |
| | Lacunar infarcts, n (%) | 6/42 (14.3) |
| | Lobar microbleeds, n (%) | 1/40 (2.5) |
| | Deep microbleeds, n (%) | 6/40 (15) |
| | Cortical superficial siderosis, n (%) | 0 (0) |

Data for microbleeds and cortical superficial siderosis missing from 2 participants. IQR indicates interquartile range; and WMH, white matter hyperintensities.

*Eight participants overlapped between the study and watershed cohorts.

**Table 2.**

Univariate Analyses and Linear Regression Models for WMH and DTI FA and MD

| | Univariate analyses | | | Multivariate linear regression | | |
|---|---|---|---|---|---|---|
| **Outcome variable** | **Predictor variable** | **Spearman *P* or directionality** | ***P* value** | **Unstandardized β (95% CI)** | ***P* value** | **Model $R^2_{adj}$; *P* value** |
| Normalized WMH volume | White matter CBF | NS | 0.432 | | | 0.697; <0.001 |
| | Watershed CBF | NS | 0.205 | | | |
| | White matter OEF ratio * | 0.740 | <0.001 | | | |
| | Watershed OEF ratio * | 0.646 | <0.001 | 0.207 (0.119 to 0.295) | <0.001 | |
| | Age * | 0.654 | <0.001 | | | |
| | Hypertension * | Higher | <0.0001 | 0.018 (0.010 to 0.025) | <0.001 | |
| | Diabetes * | Higher | 0.001 | | | |
| | Hyperlipidemia * | Higher | 0.072 | | | |
| | Race | NS | 0.558 | | | |
| | Sex | NS | 0.334 | | | |
| DTI FA | White matter CBF | NS | 0.776 | | | 0.303; <0.001 |
| | Watershed CBF | NS | 0.362 | | | |
| | White matter OEF ratio * | −0.431 | 0.004 | | | |
| | Watershed OEF ratio * | −0.455 | 0.002 | −0.243 (−0.445 to −0.041) | 0.020 | |
| | Age | NS | 0.332 | | | |
| | Hypertension * | Lower | 0.002 | | | |
| | Diabetes * | Lower | 0.005 | −0.022 (−0.043 to −0.001) | 0.041 | |
| | Hyperlipidemia | NS | 0.459 | | | |
| | Race * | NS, Black race lower | 0.027 | | | |
| | Sex * | Male lower | 0.044 | | | |
| DTI MD | White matter CBF | NS | 0.227 | | | 0.423; <0.001 |
| | Watershed CBF * | −0.264 | 0.087 | | | |
| | White matter OEF ratio * | 0.504 | 0.001 | | | |

| Outcome variable | Univariate analyses | | | Multivariate linear regression | | |
|---|---|---|---|---|---|---|
| | **Predictor variable** | **Spearman *P* or directionality** | ***P* value** | **Unstandardized β (95% CI)** | ***P* value** | **Model $R^2_{adj}$; *P* value** |
| | Watershed OEF ratio * | 0.496 | 0.001 | 0.326 (0.041–0.611) | 0.026 | |
| | Age * | 0.256 | 0.101 | | | |
| | Hypertension * | Higher | <0.001 | 0.037 (0.014–0.061) | 0.002 | |
| | Diabetes * | Higher | 0.020 | | | |
| | Hyperlipidemia | NS | 0.440 | | | |
| | Race | NS | 0.342 | | | |
| | Sex * | Male higher | 0.044 | | | |

References for the categorical variables: absence of hypertension, diabetes, hyperlipidemia, race self-identified White, and sex self-identified female. CBF indicates cerebral blood flow; DTI, diffusion tensor imaging; FA, fractional anisotropy; MD, mean diffusivity; NS, not significant; OEF, oxygen extraction fraction; and WMH, white matter hyperintensities.

*$P$<0.20 threshold for entry into the linear regression.